Title

Multispectral near-infrared reflectance and transillumination imaging of occlusal carious lesions: variations in lesion contrast with lesion depth

Authors

Simon, Jacob C
Curtis, Donald A
Darling, Cynthia L
et al.

Publication Date

2018

DOI

10.1117/12.2296013

Peer reviewed

HHS Public Access

Author manuscript

Proc SPIE Int Soc Opt Eng. Author manuscript; available in PMC 2018 February 27.

Published in final edited form as:

Proc SPIE Int Soc Opt Eng. 2018 ; 10473: . doi:10.1117/12.2296013.

Multispectral near-infrared reflectance and transillumination imaging of occlusal carious lesions: Variation in lesion contrast with lesion depth

Jacob C. Simon, **Donald A. Curtis**, **Cynthia L. Darling**, and **Daniel Fried**

University of California, San Francisco, San Francisco, CA 94143-0758

Abstract

In vivo and *in vitro* studies have demonstrated that near-infrared (NIR) light at λ=1300–1700-nm can be used to acquire high contrast images of enamel demineralization without interference of stains. The objective of this study was to determine if a relationship exists between the NIR image contrast of occlusal lesions and the depth of the lesion. Extracted teeth with varying amounts of natural occlusal decay were measured using a multispectral-multimodal NIR imaging system which captures λ=1300-nm occlusal transillumination, and λ=1500–1700-nm cross-polarized reflectance images. Image analysis software was used to calculate the lesion contrast detected in both images from matched positions of each imaging modality. Samples were serially sectioned across the lesion with a precision saw, and polarized light microscopy was used to measure the respective lesion depth relative to the dentinoenamel junction. Lesion contrast measured from NIR cross-polarized reflectance images positively correlated ($p<0.05$) with increasing lesion depth and a statistically significant difference between inner enamel and dentin lesions was observed. The lateral width of pit and fissures lesions measured in both NIR cross-polarized reflectance and NIR transillumination positively correlated with lesion depth.

Keywords

near-IR imaging; occlusal carries; detection; reflectance; transillumination; multimodal

1. INTRODUCTION

The most recent epidemiological data gathered from the National Health and Nutritional Survey (NHANES) [1, 2] and Dental Practice-Based Research Network (DPBRN) [3–5] indicates that nearly one third of all patients have a questionable occlusal carious lesion (QOC) located on a posterior tooth. QOC's are given the name "questionable" because clinicians' lack instrumentation capable of measuring the depth of pit and fissure lesions and determining if the dental decay has reached the underlying dentin. Digital x-rays are not sensitive enough to occlusal lesions, and visible diagnosis is confounded by stain trapped in the occlusal anatomy. A clinical study we performed in 2017 demonstrated that near infrared (NIR) reflectance images at λ=1500–1700 nm yielded significantly higher contrast of the

Correspondence to: Daniel Fried.

demineralization in the occlusal grooves compared with visible reflectance imaging. Stains in the occlusal grooves reduced the lesion contrast in the visible range yielding negative values on average. Additionally, only half of 26 lesions diagnosed as carious lesions and requiring restoration showed the characteristic surface demineralization and increased reflectivity below the dentinoenamel (DEJ) in 3D CP-OCT images indicative of lesion penetration into the dentin [6]. These results indicated that near infrared imaging holds great potential for the assessment of occlusal lesion depth, due to the high transparency of enamel and stain at λ=1300–1700-nm, which allows direct visualization and quantified measurements of enamel demineralization.

The development of NIR imaging has produced three distinct imaging modalities that have been tested *in vivo* and directly compared against digital x-rays on matched teeth [7–10]. These three modalities namely, cross-polarized reflectance, interproximal transillumination and occlusal transillumination were built into hand held intraoral probes and acquire high resolution diagnostic images of teeth by capturing light ranging from λ=1300–1700-nm with an InGaAs camera [7]. Previous *in vitro* studies demonstrated that images from this spectral region provides the greatest contrast between sound and demineralized enamel due to marked changes in the tissues optical properties that occur upon enamel demineralization [11].

The data collected from these clinical studies demonstrated that despite NIR imaging's superior performance in detecting early occlusal decay, NIR reflectance measurements alone are limited in utility for assessing occlusal lesion depth beyond >200-μm due to light attenuation from the lesion body [7, 12]. Additionally, both NIR reflectance and occlusal transillumination were valuable in combination for the identification of potential false positives when used for subjective diagnosis by a trained clinician. Prior *in vitro* studies attempted to combine NIR reflectance and transillumination measurements taken at λ=1300-nm in order to estimate QOC depth [13, 14]. Since, multispectral NIR reflectance and transillumination experiments have demonstrated that the tooth appears darker at wavelengths coincident with increased water absorption, multispectral images can be used to produce increased contrast between different tooth structures such as sound enamel and dentin, dental decay and composite restorative materials [15–17]. Combining measurements from different NIR imaging wavelengths and comparing them with concurrent measurements acquired by complementary imaging modalities should provide improved assessment of lesion depth and severity.

The objective of this study was to quantify the relationship between lesion contrast and lesion depth using a new imaging system that combines multispectral NIR reflectance and occlusal transillumination imaging modalities into a single device for the imaging of QOC's.

2. MATERIALS and METHODS

2.1 Sample Preparation

Posterior teeth (n=37) were selected with sound or demineralized occlusal grooves/surfaces for participation in this study. Teeth were collected from patients in the San Francisco Bay area with approval from the UCSF Committee on Human Research. The teeth were

sterilized using gamma radiation and stored in 0.1% thymol solution to maintain tissue hydration and prevent bacterial growth. Samples were mounted in black orthodontic resin in order to facilitate repeatable imaging angle and orientation.

2.2 Visible Images

A Dino-Lite digital microscope, Model 5MP Edge AM7915MZT, AnMO Electronics Corp. (New Taipei City, Taiwan) equipped with a visible polarizer was use used to acquired visible images of all samples. The digital microscope captures 5 mega-pixel (2952 × 1944) color images. Eight white LED lights contained in the camera illuminate the sample and a single polarization element in utilized to help reduce glare.

2.3 Combined NIR Occlusal Transillumination and Cross-Polarized Reflectance Imaging System

A high sensitivity, InGaAs, SWIR camera (SU640CSX) from Sensors Unlimited (Princeton, NJ), with a 320×256-pixel focal plane array and 12.5-μm pixel pitch was used to capture NIR cross-polarized reflectance and occlusal transillumination images of posterior teeth *in vitro* [18, 19]. Sample images were illuminated with filtered light from a two broadband tungsten halogen lamps (E Light) delivered through separate reflectance and transillumination fiber optic cable bundles. Reflectance illumination was achieved using a ring light from Volpi (Auburn, NY) equipped with a toroidal NIR linear polarizer custom made from a 3×3-inch polarizing sheet (Edmund Scientific, Barrington, NJ). Occlusal transillumination used a quadfurcated fiber optic bundle to deliver unpolarized light angled apically at the cementoenamel junction from both sides (buccal/lingual) of the tooth. The near-IR camera lens system was equipped with an orthogonal linear polarizer form Thorlabs (Newtown, NJ) to produce cross-polarized reflectance images with greatly reduced specular reflection.

The outputs of both broadband light sources were filtered with optical filters housed in a two motorized filter wheels, FW102 from Thorlabs. The reflectance filter wheel contained long pass λ=1500-nm filters from Spectragon (Parsippany, NJ) and the occlusal transillumination filter wheel contained long pass λ=1200-nm from Thorlabs. Each filter wheel also contained an aluminum disk (3-mm thick) used to block the light source providing on/off functionality to the multimodal system. Detailed schematics covering the geometry of each modality and theory of the resulting image contrast can be found in previous publications [18, 19]. Image data (12-bit) was delivered over a camera link cable to a Real Time PXIe-1071 chassis with NI-8133 embedded controller and NI-1428 frame grabber from National Instruments (Austin TX). A host computer, iMac (Retina 5K, 27-inch, Late 2015) from Apple (Cupertino, CA) running bootcamp and Windows 10 is used to control the Real Time PXIe.

2.4 Sectioning and Polarized Light Microscopy (PLM)

Samples were serially sectioned into ~200-μm thick slices using a linear precision saw, Isomet 5000 from Buehler (Lake Buff, IL). Thin sections containing the pit or fissure of interest were subjected to histological examination. Polarized light microscopy (PLM) was used for histological examination using a Meiji Techno RZT microscope (Saitama, Japan) with integrated digital camera, Canon EOS Digital Rebel XT (Tokyo, Japan). Sample

sections ~200-μm thick were imbibed in deionized water and examined in the bright field mode with crossed-polarizers and a red I plate (500-nm retardation).

Lesions were examined and classified according to the lesion depths: (E1) less than halfway through the enamel thickness, (E2) more than halfway through the enamel thickness, and (D) penetrating to the dentinoenamel junction. The actual lesion depth and the percent penetrance (lesion depth/enamel thickness) was measured using a standard reticle slide and image analysis package, IgorPro from Wavemetrics (Lake Oswego, OR).

2.5 Near infrared image analysis

The lesion contrast was calculated for a single carious region of interest (ROI) matched on registered reflectance and transillumination images. The image analysis package in IgorPro was utilized to extract image line profiles 10-pixels in width through the ROI. The maximum (reflectance) or minimum (transillumination) value from the image line profile was used to calculate the lesion contrast with the formulas: reflectance = $(I_L - I_S)/ I_L$ and transillumination = $(I_S - I_L)/ I_S$. These formulas normalize the percent contrast from 0–1. The lesion width was measured using the Spatial Measurement package in Igor Pro. Measurements of the lesion were acquired in the direction perpendicular to the direction of the groove in order to determine the lateral spread of the lesion.

2.6 Statistical Analysis

InStat statistical software from GraphPad (San Diego, CA) was used for one-way analysis of variance (ANOVA) followed by the Tukey-Kramer post-hoc multiple comparison test.

3. RESULTS and DISCUSSION

Natural extracted human posterior teeth (n=37) were imaged in cross-polarized reflectance from λ=1500–1700-nm and with occlusal transillumination from λ=1200–1700-nm *in vitro* using a multimodal-multispectral imaging apparatus equipped with an InGaAs camera. Samples were serially sectioned with a precision wet saw and analyzed for enamel lesion depth with polarized light microscopy (PLM). An independent examiner blinded to the NIR sample images utilized PLM data to stratify the lesions by depth into E1-outer half of enamel (n=7), E2-inner half of enamel (n=11), and D-penetrating into dentin (n=19) (Table 1). Sample lesion depths were measured using PLM images yielding group averages of E1=0.33±0.19-mm, E2=1.19±0.27-mm, and D=1.62±0.32-mm. To account for the limitation that PLM lesion depths are only reliable through the enamel a metric termed, "lesion penetrance" was calculated by dividing the measured lesion depth by the enamel depth at the analyzed location to scale the lesions from 1–100%.

The stratified mean lesion penetrance values are shown in Table 1.

The lesion contrast measured from NIR images was calculated by relating the intensity of sound tooth structure (I_S) to the intensity of the suspected lesion (I_L) using the formulas: reflectance = $(I_L - I_S)/ I_L$ and transillumination = $(I_S - I_L)/ I_S$. IS was calculated using two different methods for NIR reflectance. The traditional method (sound) uses the mean intensity from a region enamel on an unaffected surface that is hand selected by the operator

using image processing software. An alternative method (total) utilizes all the pixels from the tooth and is therefore easily automated. The total method was previously proven capable of calculating contrast values in real time and it uses an image processing algorithm to isolate the tooth occlusal surface from its surroundings, and calculate the mean intensity of all pixels contained within the sample [19]. The mean contrast in reflectance calculated using both methods is shown in Table 1. The performance of the total method is as successful as the traditional method for early enamel occlusal lesions but as the lesion depth and size increases, the contrast plateaus due to the fact that the fraction of pixels defining the lesion increases for the total mean value set. The total method demonstrated a statistically significant difference in the lesion contrast between E1 and D depth lesions. The sound method demonstrated a statistically significant difference in the lesion contrast between E2 and D depth lesions. Transillumination mean contrast values calculated using the sound method are presented in Table 1. No differences in lesion contrast among the stratified samples were detected.

The size of the lesion detected in the NIR reflectance and transillumination images was measured as the pixel quantity in the dimension perpendicular to the occlusal groove or as a circular diameter in the affected occlusal pit. The lesion boundary was defined as the pixel where the lesion contrast was less than 10% contrast. Both NIR reflectance and transillumination images demonstrated a statistically significant difference in the lesion width between E2 and D depth lesions (Table 1).

Tooth samples were then analyzed based on their measured lesion depths to determine the relationship in lesion contrast as a function of absolute lesion depth in the occlusal-apical (top-bottom) dimension. Figure 1 is a graph of the NIR reflectance contrast for both sound and total calculation methods compared to the measured lesion depths. Regression lines for each method are statistically significant ($P<0.05$). The sound method typically yields a higher contrast value compared to the total method. The plot demonstrates that NIR reflectance from λ=1500–1700-nm is more likely to underestimate the lesion size, most likely due to water absorption within the lesion.

Additionally, there was a sharp increase in lesion contrast when the lesion was greater than 1-mm in depth.

Figure 2 shows the NIR transillumination contrast for sound, total and occlusal calculation methods compared to the measured lesion depths. The occlusal calculation method is analogous to the sound method but it samples a region within the occlusal table where the dentin underlies the sound enamel. The regression lines for each method were not statistically significant. The lack of significance is most likely due to the high contrast values measured from sound (lesion depths<0.25-mm) samples which can be seen on the left side of Fig. 2. Even though the groves and fissures of the occlusal anatomy are small in width, they are dark relative to the surrounding sound tooth enamel.

The lateral width of the lesion correlated ($P<0.05$) with the lesion depth for the NIR cross-polarized reflectance and transillumination images (Fig. 3). This result is consistent with our

findings in other OCT studies where we were able to measure the lateral spread of occlusal lesions when they reached the dentinoenamel junction [6, 9, 20].

In summary, the lesion contrast measured from NIR cross-polarized reflectance images positively correlated ($P<0.05$) with increasing lesion depth and a statistically significant difference between inner enamel and dentin lesions was observed. The lateral width of pit and fissures lesions measured in both NIR cross-polarized reflectance and NIR transillumination positively correlated with lesion depth.

Acknowledgments

This work was supported by the NIH/CNIDCR Grants R01-D14698 and F30-DE026052.

References

1. Dye B, Thornton-Evans G, Li X, Iafolla T. Dental caries and tooth loss in adults in the United States, 2011–2012. NCHS data brief. 2015; (197):1–8.
2. Dye BA, Tan S, Smith V, Lewis BG, Barker LK, Thornton-Evans G, Eke PI, Beltran-Aguilar ED, Horowitz AM, Li CH. Trends in oral health status: United States, 1988–1994 and 1999–2004. Vital and health statistics Series 11, Data from the National Health Survey. 2007; 248:1–92.
3. Makhija SK, Gilbert GH, Funkhouser E, Bader JD, Gordan VV, Rindal DB, Pihlstrom DJ, Qvist V. P. C. G. National Dental. Characteristics, detection methods and treatment of questionable occlusal carious lesions: findings from the national dental practice-based research network. Caries Res. 2014; 48(3):200–7. [PubMed: 24480989]
4. Makhija SK, Gilbert GH, Funkhouser E, Bader JD, Gordan VV, Rindal DB, Qvist V, Norrisgaard P. P. C. G. National Dental. Twenty-month follow-up of occlusal caries lesions deemed questionable at baseline: findings from the National Dental Practice-Based Research Network. J Am Dent Assoc. 2014; 145(11):1112–8. [PubMed: 25359642]
5. Makhija SK, Gilbert GH, Funkhouser E, Bader JD, Gordan VV, Rindal DB, Bauer M, Pihlstrom DJ, Qvist V. G. National Dental Practice-Based Research Network Collaborative. The prevalence of questionable occlusal caries: findings from the Dental Practice-Based Research Network. J Am Dent Assoc. 2012; 143(12):1343–50. [PubMed: 23204090]
6. Simon JC, Kang H, Staninec M, Jang AT, Chan KH, Darling CL, Lee RC, Fried D. Near-IR and CP-OCT imaging of suspected occlusal caries lesions. Lasers Surg Med. 2017; 49(3):215–224. [PubMed: 28339115]
7. Simon JC, Chan KH, Darling CL, Fried D. Multispectral near-IR reflectance imaging of simulated early occlusal lesions: variation of lesion contrast with lesion depth and severity. Lasers Surg Med. 2014; 46(3):203–15. [PubMed: 24375543]
8. Fried D, Staninec M, Darling CL, Kang H, Chan K. In vivo Near-IR Imaging of Occlusal Lesions at 1310-nm. Lasers in Dentistry XVII. Proc SPIE. 2011; 7884 B:1–7.
9. Staninec M, Douglas SM, Darling CL, Chan K, Kang H, Lee RC, Fried D. Nondestructive Clinical Assessment of Occlusal Caries Lesions using Near-IR Imaging Methods. Lasers Surg Med. 2011; 43(10):951–959. [PubMed: 22109697]
10. Staninec M, Lee C, Darling CL, Fried D. In vivo near-IR imaging of approximal dental decay at 1,310 nm. Lasers Surg Med. 2010; 42(4):292–8. [PubMed: 20432277]
11. Darling CL, Huynh GD, Fried D. Light scattering properties of natural and artificially demineralized dental enamel at 1310 nm. J Biomed Opt. 2006; 11(3):34023. [PubMed: 16822072]
12. Chung S, Fried D, Staninec M, Darling CL. Near infrared imaging of teeth at wavelengths between 1200 and 1600 nm. Lasers in Dentistry XVII. Proc SPIE. 2011; 7884 X:1–6.
13. Lee C, Darling CL, Fried D. In vitro near-infrared imaging of occlusal dental caries using a germanium enhanced CMOS camera. Lasers in Dentistry XVI. Proc SPIE. 2010; 7549 K:1–7.

14. Lee C, Lee D, Darling CL, Fried D. Nondestructive assessment of the severity of occlusal caries lesions with near-infrared imaging at 1310 nm. J Biomed Opt. 2010; 15(4):047011, 1–8. [PubMed: 20799842]
15. Zakian C, Pretty I, Ellwood R. Near-infrared hyperspectral imaging of teeth for dental caries detection. J Biomed Opt. 2009; 14(6):064047–7. [PubMed: 20059285]
16. Tom H, Simon JC, Chan KH, Darling CL, Fried D. Near-infrared imaging of demineralization under sealants. J Biomed Opt. 2014; 19(7):77003. [PubMed: 25036214]
17. Simon JC, Lucas S, Lee R, Darling CL, Staninec M, Vanderhobli R, Pelzner R, Fried D. Near-infrared imaging of natural secondary caries. Lasers in Dentistry XXI. Proc SPIE. 2015; 9306, F: 1–8.
18. Simon JC, Darling CL, Fried D. A system for simultaneous near-infrared reflectance and transillumination imaging of occlusal carious lesions. Lasers in Dentistry XXII. Proc SPIE. 2016; 9692 A:1–6.
19. Simon JC, Darling CL, Fried D. Assessment of cavitation in artificial approximal dental lesions with near-IR imaging. Lasers in Dentistry XXIII. Proc SPIE. 2017; 1004 7:1–7.
20. Lee C, Lee D, Darling CL, Fried D. Nondestructive assessment of the severity of occlusal caries lesions with near-infrared imaging at 1310 nm. J Biomed Opt. 2010; 15(4):047011. [PubMed: 20799842]

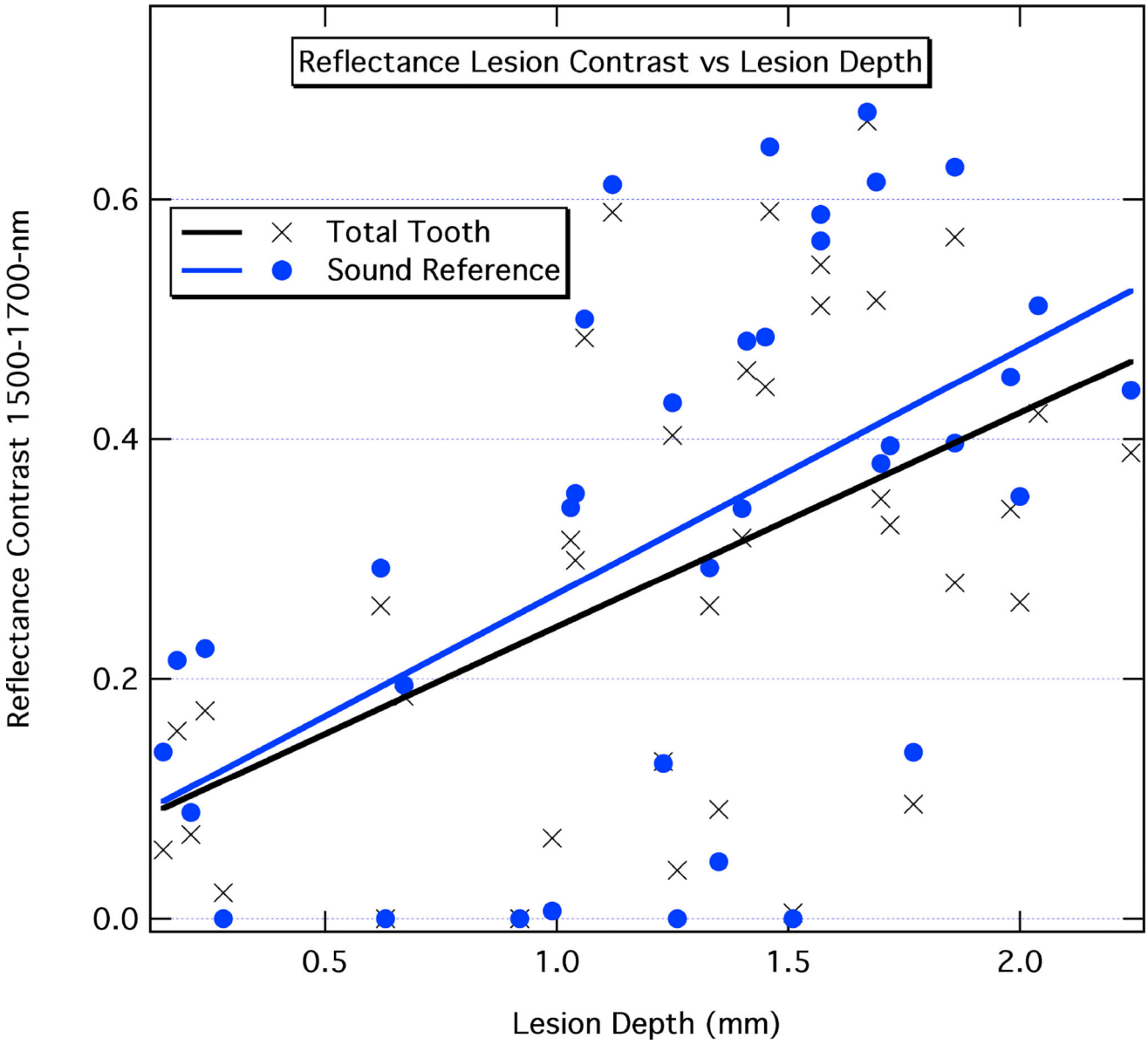

Fig. 1.

NIR reflectance contrast values vs. measured lesion depth from PLM histology. Blue circles and the blue regression line represent contrast values from the traditional (sound) method. Black (X) symbols and the black regression line represent contrast values from the automated (total) method. Both regressions are statistically significant ($P<0.05$).

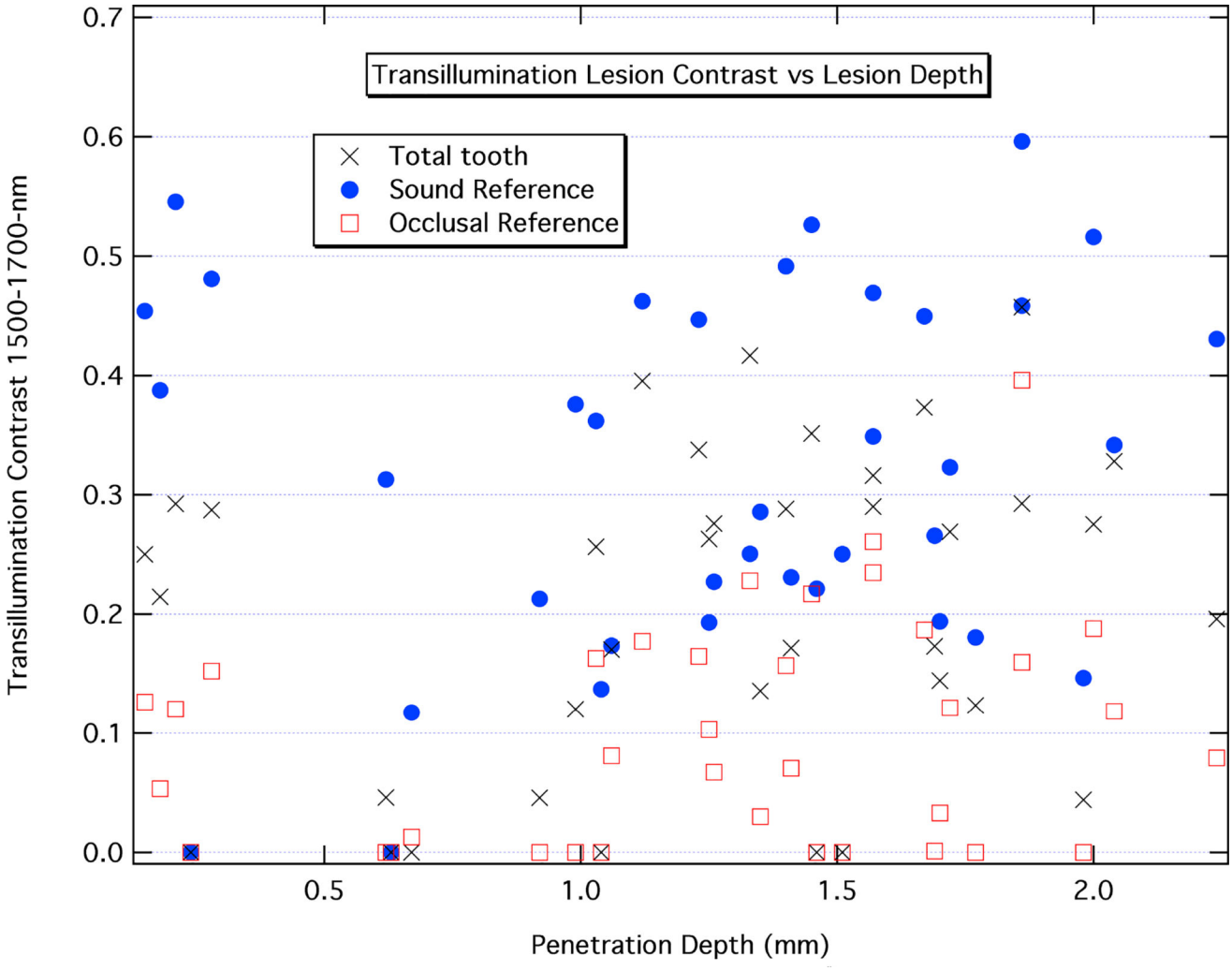

Fig. 2.

NIR transillumination contrast vs. measured lesion depth acquired from PLM histology. Blue circles represent contrast values from the traditional (sound) method. Black (X) symbols represent contrast values from the automated (total) method. Red boxes represent values from the occlusal method. Individual regression calculations showed no statistical significance (P>0.05).

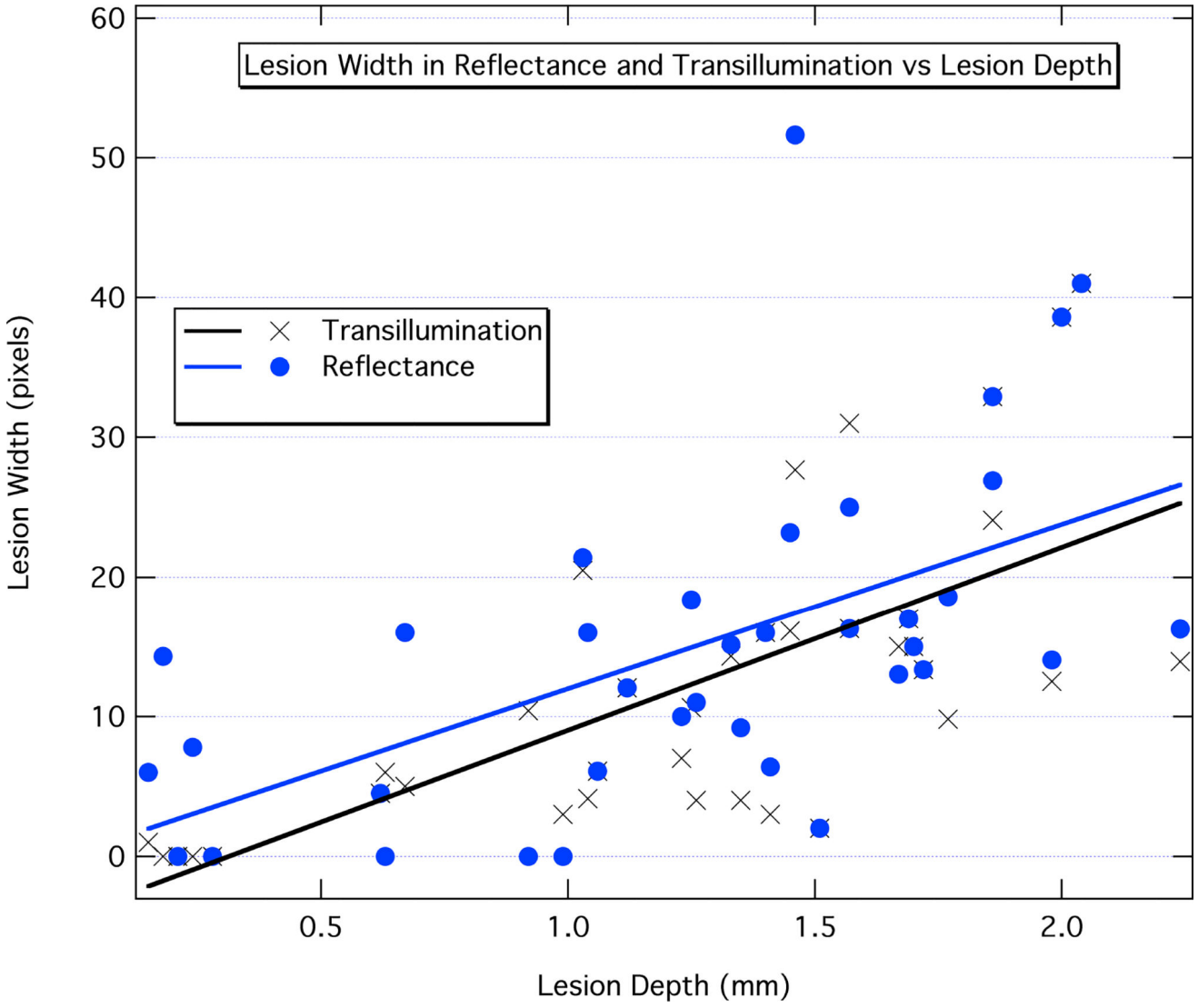

Fig. 3.

NIR reflectance and transillumination lesion widths vs. measured lesion depth from PLM histology. Blue circles represent reflectance measurements. Black (X) symbols represent transillumination measurements. Both regressions are statistically significant ($P<0.05$).

Table 1

Sample population statistics stratified by lesion depth into E1(<50% enamel), E1(>50% enamel), and D(dentin) depths (column 1–4). Lesion contrast values for NIR reflectance λ=1500–1700-nm are presented for two calculation methods, "total" and "sound" (column 5–6). Lesion contrast values for NIR transillumination λ=1200–1700-nm are shown for the “sound” method (column 7). The mean lesion width measured in pixels (column 8–9). Letters represent statistical grouping based on ANOVA.

Lesion Category	Sample Size	Mean Lesion Depth (mm)	Mean Lesion Penetrance	Mean Reflectance Contrast (total)	Mean Reflectance Contrast (sound)	Mean Transillumination Contrast (sound)	Mean Reflectance Lesion Width (pixels)	Mean Transillumination Lesion Width (pixels)
E1	7	0.33 ± 0.19	28.3% ± 13.6	10.6% ± 8.71 a	13.7% ± 11.4 a	31.2% ± 20.8 a	4.65 ± 5.31 a	1.6 ± 2.53 a
E2	11	1.19± 0.27	77.9% ± 9.72	24.7% ± 20.6 a,b	24.8% ± 23.7 a	26.2% ± 10.9 a	8.8 ± 6.43 a	7.10 ± 4.3 a
D	19	1.63 ± 0.32	100%	28.3% ± 15.4 b	43.5% ± 16.8 b	35.8% ± 13.3 a	22.4 ± 11.2 b	19.4 ± 10.6 b